Dark Pixel Detection: A Novel Single Image Dehaze Approach

Qi Yu *
School of Applied Mathematics
ZheJiang University
yuqirose@zju.edu.cn

Zhihao Ding*
School of Computer Science
ZheJiang University
cuanding@zju.edu.cn

RongRong
walterddr@gmail.com

Zhenyue Zhang
and Donghui Wang
{zyzhang,dhwang}@zju.edu.cn

Abstract—In this paper, we introduce a simple but effective method in order to remove haze in foggy images. We name it as dark pixel detection. Dark pixel is the pixel in haze-free images with values in all of the RGB colour channels close to zero. With this method, we can effectively estimate the thickness of the haze and recover a vivid haze-free scene even when the scene object is inherently similar to the air light across a large region. In addition, our algorithm is fast and with good dehazing quality.

Index Terms—computer vision, image process, dark pixel detection, dehaze

I. INTRODUCTION

Images taken in the environment with heavy fog, haze and smoke are characterized by lower saturation, poor contrast and additional noise. Fog, haze and smoke all consist of a multitude of tiny particles. On a clear day, light reflected from the scene directly reaches the camera, while in bad weather light would be partly absorbed and scattered by the particles along the line of sight. In addition, the reflected light would be blended with the airlight [8] which is reflected by these particles. The longer the distance between the scene and the camera, the more the degradation occurs.

Haze removal is critical for a wide range of image-related applications, such as surveillance systems, intelligent vehicles, satellite imaging, and outdoor object recognition systems. Besides, the by-product of haze removaldepth information is desired in design of many vision algorithms.

However, enhancing the visibility of haze images is not a trivial work because haze removal is an ill-posed problem. The optical model describing the effect of the fog on a haze image is as follows [8]:

$$I(x) = R(x)t(x) + A(1 - t(x)) \qquad (1)$$

where I is the observed light intensity vector with values in RGB three channels, R is the scene radiance vector, A is the constant airlight vector, x is the position of the scene point and t is the transmission along the line of sight which is the same in each of the three channels.

In homogeneous atmosphere, the transmission t can be expressed as

$$t(x) = e^{-r*d(x)} \qquad (2)$$
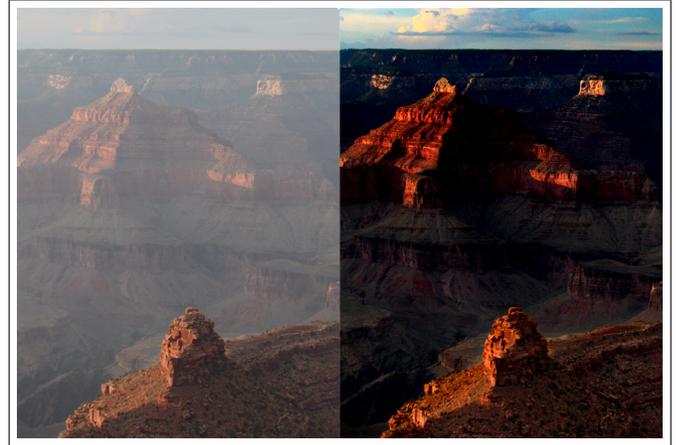
Fig. 1. Example of dehazed image using dark pixel detection Left: input haze image, Right: our result

where r is the scattering attenuation coefficient of the atmosphere and d is the scene depth. Equation (1) demonstrates that the light received by the camera I is in a convex combination of two kinds of light: the direct attenuation of the scene radiance R and the constant airlight A. To obtain the haze-free image, we need to determine the unknown constant A and the transmission $t(x)$.

In this paper, we propose a novel approach to solve single image dehaze problem. Our core technique is a fast detection of dark pixels whose scene radiances are close to zero even when they are covered by heavy haze. The transmission of these pixels can be directly computed according to the haze equation. Then we use these known transmissions to estimate other unknown pixels. We segment the image into different blocks according to depth-related information and apply two-dimension curved surface fitting in each block according to the known transmissions. Shortly after a fast smooth filtering, the whole transmission map, the set of all the $t(x)$ in the image, becomes available. Figure 1 is a implementation example of our approach.

Our approach depends on no prior or assumption. While all of the current approaches fail when the image mismatches their prior or assumption, our approach shows stable performance.In particular, they all bump into trouble processing an image with a large region whose color is similar to the air light while our

method still works well, see Figure 4 for example. Thanks to the size-controlled segmentation step, the recovered image would not suffer halo artefacts at the depth-discontinuous edges. Moreover, our algorithm performs fast, being suitable for real-time applications.

II. RELATED WORK

Since the haze removal problem is ill-posed, additional information should be retrieved for haze removal generally. Some techniques utilize multiple images of the same scene [9] [10] or near-infrared image [11]. In [16], a rough estimation of the depth function $t(x)$ should be given under user assistance. Kopf et al. applies the existing geo-referenced digital terrain and urban models [13]. It's inconvenient to use these methods because besides the input image, more information has to be gathered.

Recently, several haze-removal methods for single image have been proposed. Each method relies on a different assumption or prior, showed in table I.

TABLE I
DEHAZE APPROACH PRIOR/ASSUMPTION

Fattal [1]	Image shading and transmission are locally uncorrelated
Kratz Nishino [5]	The albedo and depth are statistically independent
Zhang et al [6]	Large-scale chromaticity variations are due to transmission while small-scale luminance variations are due to scene albedo
Peter [7] Hartley	Objects appearing towards the top of the image are usually further away
He et al [3]	Most local patches in haze-free outdoor images contain some pixels which have very low intensities in at least one color channel.
Tan [2]	Contrast should be maximized in haze-free image

However, as authors describe in their papers, their methods fail in some cases respectively when the assumptions or prior do not hold. One of their common drawbacks is transmission estimating failure when the relative proportion of the RGB values of the scene, over a large compact region, is inherently similar to that of the airlight. Typical examples are the grey surface of a highway and a white wall. This happens because the proportion of their RGB channel values approximates 1:1:1, which resembles that of the airlight.

A. Dark Pixel Detection

Dark-object subtraction is one of the basic methods in remote sensing for haze removal [12] . Dark object is an object that reflects little light. When a dark object is found, spatial-homogeneous haze can be removed by subtracting a constant value corresponding to this object. However, this method needs users to choose the dark object in the image. Another drawback is that when coming across images with spatial-variant haze, this method fails. In this paper, we generalize this subtraction idea, using an automated alternative.

In fact, the nature is full of shadows, which is also a kind of dark object. The appearance of shadow is due to obstruction of light by some object. Generally, an image that needs haze removal has a deep depth of field, which implies there are a multitude of objects in the images. Since the sun is an approximately parallel light source, these objects in the scene become shelters for areas nearby and produce lots of shadows. Because of these shadows and other inherently dark objects, we could find a large number of widespread dark pixels in the image.

We observe that dark pixels, either in haze-free images or in hazy images, have two characteristics which we regard as conditions for selection:

1) Channel Transformation: The color of the dark pixel in the input image is non-pure under white light source no matter how heavy the haze is, because the colors of both the scene radiance of the dark object and the haze are non-pure. If we transform I from RGB space into YC_bC_r space, both C_b and C_r of dark pixels are close to 128, where C_b and C_r range from 16 to 240. In our algorithm, this condition is expressed as.

$$(C_b - 128)^2 + (C_r - 128)^2 < \theta \qquad (3)$$

2) Neighboring Domain : The dark pixel has a smaller luminance than pixels in its neighboring domain unless some of them are also dark pixels. To avoid false positive result, a stricter condition is performed that the largest value in RGB channels of the target pixel must be smaller than the minimum values in RGB channels of its neighboured pixels. To reduce computation cost, we merely choose four representative pixels nearby: each pixel, 10 pixels the right, left, above, and below. A large set of experiment confirms the effectiveness of our method.

Before detecting dark pixels, we should guarantee that light source of the input image is white light source, so white balance is introduced ahead of detection. Since the color of haze should be white, the reference white points are chosen to be the haze-opaque region which would be discussed in section III C.

Besides, in images of low quality, some unpleasant noise may mistakenly become our target dark pixels. In this paper, we assume that all the input images have been de-noised, otherwise we employ median filter for preprocessing.

To examine the validity of our method, we collect about 200 landscape images from Flickr.com for experiment. Half of the images are haze-free while the rest are hazy. Figure 2 shows several sample images and the corresponding dark pixel distributions. The experimental results illustrate that there are a large number of dark pixels, generally ranging from 4000 to 20000, in any 480*600 input image. More importantly, these pixels are located in almost every corner in the image, which demonstrates the broad distribution of dark objects in an input image.

Since dark pixels reflect little light, the haze-free radiance R of these pixels can be treated as the zero vector. Taking minimums on both sides of Equation 1 and then doing simple algebra, we can obtain the transmissions of these pixels:
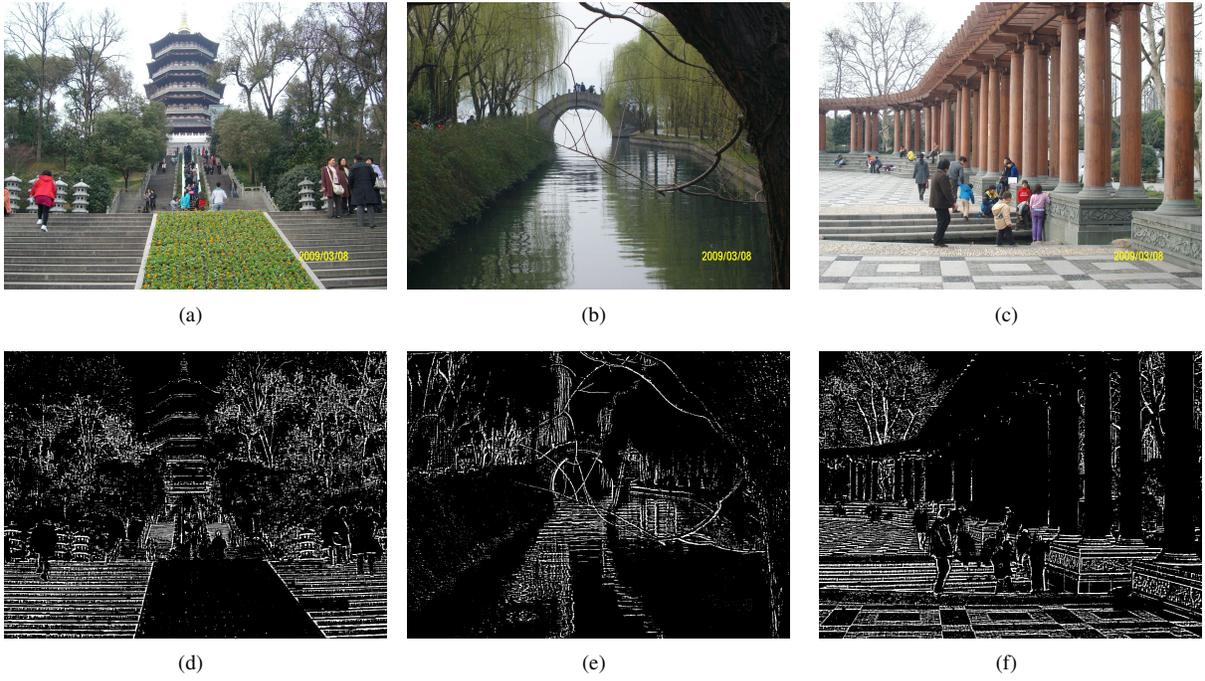
Fig. 2. Images and corresponding dark pixel maps. (a)(b)(c): Example images in our large data set. (d)(e)(f): The corresponding dark pixel distribution. Dark pixels is shown in pure white color.

$$t(x) \quad = 1 - \frac{min_{r,g,b}\{I(x)-R(x)t(x)\}}{A^c} \qquad (4)$$
$$\approx 1 - \frac{min_{r,g,b}I(x)}{A^c}$$

where $min_{r,g,b}I(x)$ is the minimal color channel of $I(x)$ and A^c is the corresponding color channel of vector A. Using the transmissions of these wide-spread dark pixels, we can estimate the transmissions of their neighboring pixels in the whole image.

B. Segmentation and 2D Fitting

Given lots of comparatively accurate dark pixel transmissions, the task of obtaining the whole transmission map becomes an interpolation or fitting problem. We employ the 2D linear fitting instead of interpolation because we observe the transmission t would not change sharply in a local area with continuous depth. Moreover, linear fitting is less computationally intensive, yielding comparable results at the same time. Regarding depth discontinuity, which affects transmission estimate accuracy to a large extent, we consider image segmentation to recognize and segment the image into various blocks before fitting. We basically adopt the algorithm of Felzenszwalb and Huttenlocher [15] for two reasons:

1) It is computationally efficient running in $O(nlogn)$ time for n image pixels
2) It can easily control the size of the blocks by merely adjusting the parameter k, being suitable for controlling the accuracy of the 2D fitting.

However, the segmentation criterion is not color. The best wish is segmenting the image according to t or the distance between the scene point and the camera, though it is impossible because t is exactly what we want and the distance is closely related to t. But according to Equation 1, if $R^c = 0$, then

$$t = 1 - \frac{I^c}{A^c} \qquad (5)$$

where c could be R, G or B color channel, indicating that t has a linear relation with I^c, and the first order coefficient $-\frac{1}{A^c}$ in each of the RGB channel is the same due to white balance. According to 1 again, to minimize $R^c(x)$ in order to maintain the approximate linear relation between t and I^c, we replace the vector I with the minimum value in the RGB channels of each pixel in the image. We called this new generated black-and-white image *dark map*. Segmentation is performed on the dark map.

After dividing the image into different blocks, we first do linear fitting in each block which contains more than 20 dark pixels for robustness: using the transmission and position values of these pixels to calculate the coefficients of the fitting formula

$$t = ax + by + c \qquad (6)$$

where x and y are horizontal and vertical coordinate, respectively. For each of the rest blocks, we choose pixels close to the block to estimate the coefficients. In our method, these pixels are chosen in the smallest rectangle containing the block on which fitting is performed. Then we employ guided image filter [14] to improve the accuracy of the rough transmission

map. We choose the dark map as the guided image and set $\epsilon = 10^{-2}$ and $r = 20$.

To achieve high level of accuracy when employing the 2D linear fitting, the size of the blocks should not be too large. Thanks to the algorithm proposed by Felzenszwalb and Huttenlocher [15] , we can set the coefficient k in the algorithm to control the block size. In our experiment, k is set 100 in a 480*600 input image to meet the requirement.

C. Airlight and Haze-Opaque Region

Apart from transmission map, the estimation of the airlight color A is also important. According to [8], A should be the color values of the scene point with infinite distance away from the camera. It can also be comprehended in this way: when the distance is infinite, $t(x) = 0$ according to Equation (2), and hence $I(x) = A$ according to Equation 1. Consequently, A can be best estimated in the most haze-opaque region. Tan [2] regard the brightest pixel as the air light, but the brightest pixel in an image may be a small white object such as a white goose or a white wall, or even be the noise. Tarel *et al* [4] apply white balance on the image and assume that A has a larger intensity than that of any other pixel. This method also encounters the problem Tan suffers.

Thanks to the size-controlled segmentation algorithm, we can avoid this problem and pick out the most haze-opaque region correctly. When the coefficient is set appropriately according to the image size, all blocks segmented are of proper size. As a result, those small pieces of pixels on the ground with brightest pure white color seldom constitute an entire block. We first compute the average value for each block in dark map. The block with the largest average value is chosen to be the haze-opaque region. Then A is estimated by the average value in each of the RGB channels in this region in the original input image.

D. Recovering the Scene Radiance

Now that the values of A and $t(x)$ are obtained, the scene radiation can be recovered by solving Equation (1) for each pixel.

$$R(x) = A - \frac{A - I(x)}{t(x)} \qquad (7)$$

But when the denominator $t(x)$ is close to zero, the error of $R(x)$ R(x) will approach infinity. Hence, a lower bound of $t(x)$ should be set. Unlike previous methods in which the lower bound of $t(x)$ remains the same in any input image, our method is image-oriented. Since the smallest $t(x)$ always appears in the haze-opaque region, we regard the largest $t(x)$ in that region as the lower bound

$$t_0 = 1 - \frac{min_\Omega I_d}{A^c} \qquad (8)$$

where Ω is the block of haze-opaque region and I_d is the value in dark map. Ultimately, the scene radiance is computed as follows:

$$R(x) = A - \frac{A - I(x)}{max\{t(x), t_0\}} \qquad (9)$$

For review, all the steps of our method are presented in order as follows. Corresponding effect image is shown in figure 3

1) Compute dark map
2) Size-controlled segmentation according to dark map
3) Target the haze-opaque region and estimate the constant airlight value
4) Detect dark pixels
5) Fit the transmission map in each block
6) Recover scene radiance

III. EXPERIMENT AND DISCUSSION

The experiments are conducted on popular images He, Fattal, Tarel and Hautiere have tested. We set the parameter k in 2D fitting as 100 and θ in Equation 3 as 10.

A. Processing Time

Using a 1.8GHz Intel 2 duo 2 Processor to process 480*600 pixel image, Table II shows the average processing time.

TABLE II
AVERAGE DEHAZE TIME

Approach	Fattal [1]	He *et al* [3]	Tarel [4]	Dark Pixel
Time(s)	385	15.26	0.17	0.1-1.5

We can find that our approach performs at the similar level to that of Tarel and Hautieres, but much faster than Fattal and He *et al*. However, Tarel and Hautieres method faces the risks of producing artifacts close to the patch transitions and thus distort the global contrast.

B. Dehaze Accuracy

Currently, most dehaze approaches suffer from a situation which is also mentioned by He *et al*. when the scene objects are inherently similar to the atmospheric light and shadow is cast on them. Dehazed white marble becomes yellow under this situation. He *et al*'s dehazing technique relies on the dark channel prior: most local patches in haze-free outdoor images contain some pixels which have very low intensities in at least one color channel.It divides the input image into 15pixel*15pixel patches and directly assumes that there is at least one such pixel in each patch. The transmission of this target pixel is calculated and used to represent the transmissions of the rest pixels in that patch. After a global smoothing step, the whole transmission map becomes available. This dehazing process implies that once the transmission of the target pixel has a wrong estimation, the whole patch suffers the same as that of an ordinary marble stone.

However, dark pixel detection overcomes it since we do not use any prior but processes alternatively: If dark pixel is detected within a block, we use it for transmit estimation. Otherwise, we ignore the block. Figure 4 displays our improvement compared with He's approach.
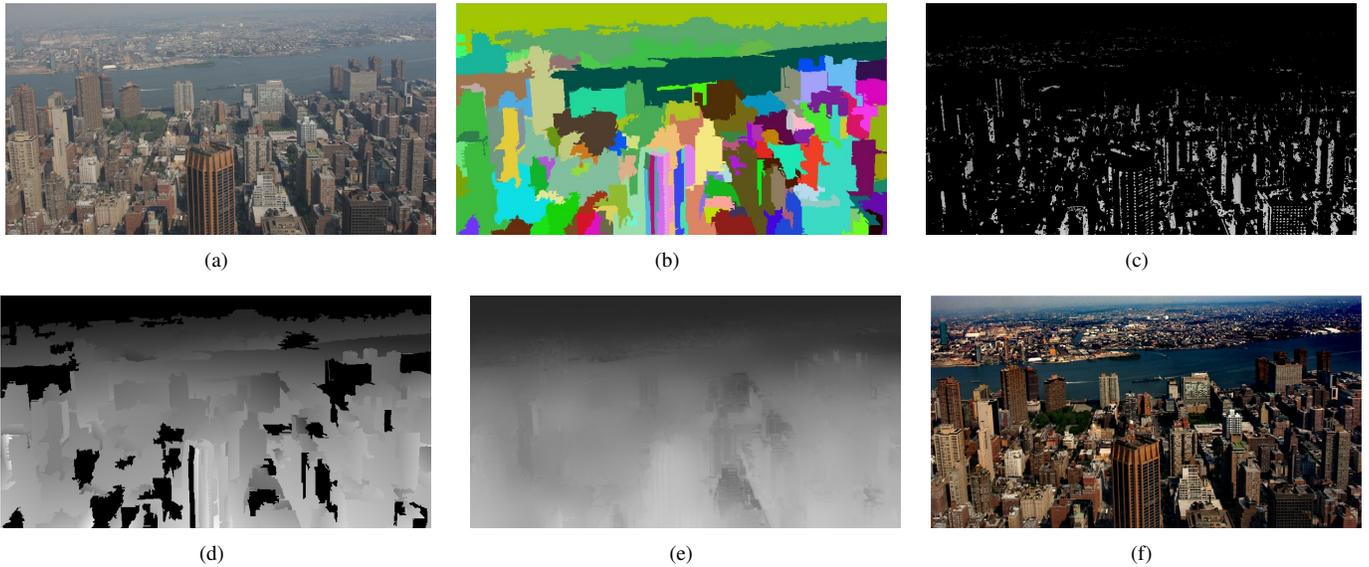
Fig. 3. Steps in conducting dark pixel detection dehaze: (a) input image; (b) segmentation step ; (c) detect dark pixels; (d) 2D linear fitting; (e) smooth for transmission map (f) our result.

Fig. 4. Comparison with He's dark channel approach: (a) input image with while marbles; (b) He *et al* [3]'s transmission map ; (c) He *et al* [3]'s result; (d) image with dark pixels; (e) our transmission map (f) our result.

Figure 4(e) is the transmission map. Note that the gradient of our transmission map is consistent with the field depth of the scene. In contrast, He's transmission map fails because people in the image should be of same depth as marbles they stand on, thus the transmission should be continuous. Our result in Figure 4(f) recover the original pure white color of marbles on the right corner of the image while He's result in Figure 4(c) makes the marble to be yellow.

C. Image Quality

To evaluate dehazed image quality, we adopted N.Hauti'ere's [17] method to compare normalized ascension of contrast degree. Table III demonstrates the result. Our approach ranks best among Fattal's and He *et al*'s. The contrast degree index values vary with images but this can be a quantitate metric of dehaze approaches. Figure 5 shows more results of dehazing approach comparison, we can conclude that our approach recovers hazed image with better colour contrast.

TABLE III
CONTRAST DEGREE

C-index	He *et al* [3]	Fattal [1]	Dark Pixel
ny12	0.8302	0.6860	1.000
ny17	0.8640	0.7024	0.9147
ny1	0.4034	0.1973	0.6603

D. Improvement

Since our method relies on segmentation, an unreasonable segmentation could yield a bad result. Background pixels in haze-opaque regions disturb our effect in some extend. As shown in Figure 6, although we recover most of the scene radiation well, the transmission of the haze-opaque region is wrong because this region includes the river whose distance from the camera is much shorter. On the left corner of the Figure 6(d), the atmosphere turns into blue, thus a failure case.

IV. CONCLUSION

In this paper, we introduce a novel dark pixel detection approach in order to remove haze in foggy images. We estimate the thickness of the haze by detecting dark pixels, segmenting blocks, fitting transmission maps, and calculating airlight. The approach is especially effective when the scene

(a)

(b)

(c)

(d)
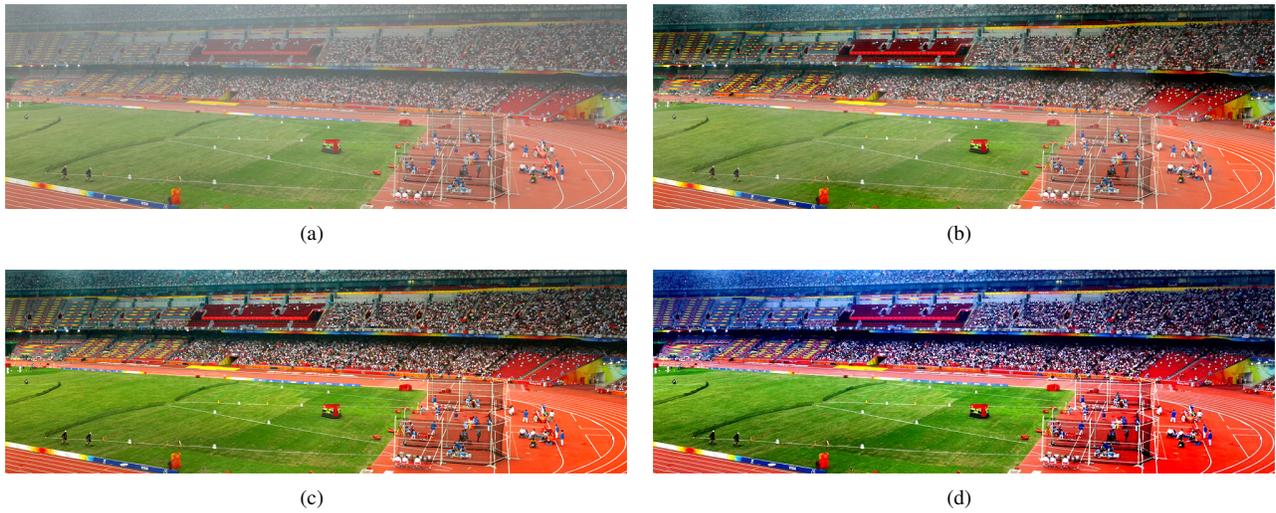
Fig. 6. Example when dark pixel detection fails the dehaze: (a) input image; (b) Fattal's [1] ; (c) He's *et. al* [3]; (d) Ours.

(a)

(b)

(c)

(d)

(e)

(f)
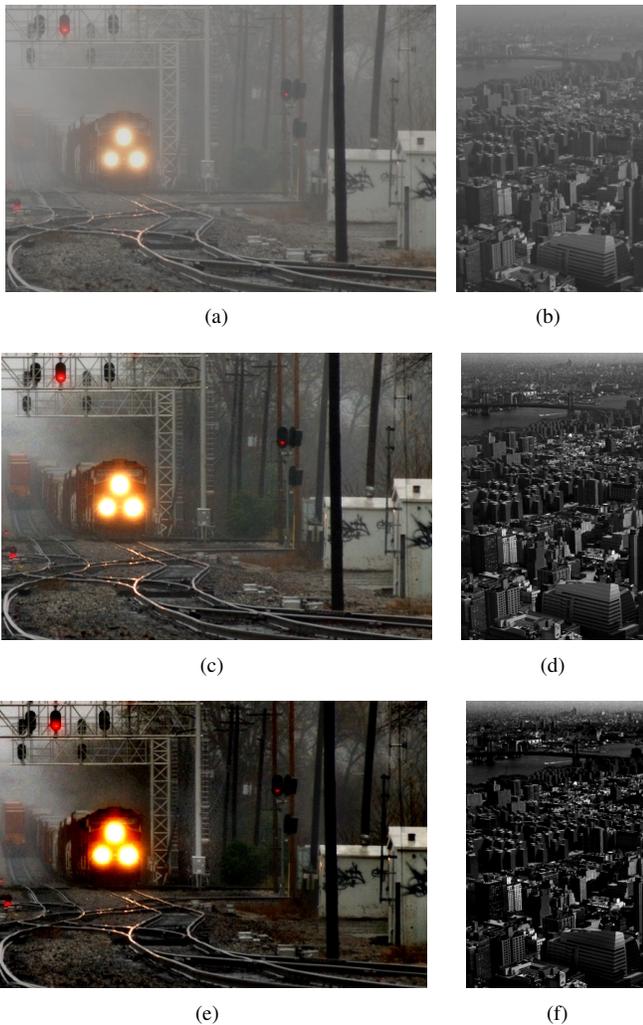
Fig. 5. More results comparison: Top: input haze image; Middle: He's result; Bottom: our result

object has similar colour to the airlight in a large area. We also experiment with the speed of the algorithm and resulting quality using existed methods. Hazed images processed by dark pixel detection recover clear vision and retain fine details, demonstrating the effectiveness and efficiency of our method.

ACKNOWLEDGMENT

REFERENCES

[1] R. Fattal, *Single image dehazing*. SIGGRAPH,2008.

[2] R. Tan, *Visibility in bad weather from a single image*. CVPR,2008.

[3] He, K., Sun, J., Tang, X, *Visibility in bad weather from a single image*. CVPR,2009.

[4] Tarel, J., Hautiere, N., *Fast visibility restoration from a single color or gray level image*. ICCV,2009.

[5] Kratz, L., Nishino, K. , *Factorizing scene albedo and depth from a single foggy image*. ICCV,2009.

[6] Zhang, J., Li, L., Yang, G., Zhang, Y. , *Local albedo-insensitive single image dehazing*. The Visual Computer. Vol. 26. 761-768, 2010.

[7] Carr, P., Hartley, R. , *Improved single image dehazing using geometry*. dicta, 103-110, 2009 Digital Image Computing: Techniques and Applications, 2009.

[8] Nayar, S., Narasimhan, S, *Vision in bad weather*. ICCV,1999.

[9] Narasimhan, S., Nayar, S., *Chromatic framework for vision in bad weather*. CVPR,2000.

[10] Narasimhan, S., Nayar, S., *Contrast restoration of weather degraded images*. PAMI,2003.

[11] Schaul, L., Fredembach, C., Ssstrunk, S, *Color image dehazing using the near-infrared*. Remote Sensing of Environment, 1988.

[12] Chavez, P, *An improved dark-object subtraction technique for atmospheric scattering correction of multispectral data*. on Image Processing, 2009.

[13] Kopf, J., Neubert, B., Chen, B., Cohen, M., Cohen-Or, D., Deussen, O., Uyttendaele, M., Lischinski, D. , *Deep photo-model-based photograph enhancement and viewing*. ACM Transactions on Graphics, 2008.

[14] He, K., Sun, J., Tang, X, *Guided image filtering*. ECCV, 2010.

[15] Felzenszwalb, P., Huttenlocher, D., *Efficient graph-based image segmentation*. International Journal of Computer Vision,59(2), 167-181, 2004.

[16] Narasimhan, S., Nayar, S, *Interactive de-wheatering of an image using physical models*. ICCV Workshop CPMVC, 2003

[17] N. Hauti'ere, J.-P. Tarel, D. Aubert, and E. Dumont, *Blind contrast enhancement assessment by gradient ratioing at visible edgee*. Image Analysis & Stereology Journal, 27(2):8795, June 2008.